Development 140, 1981-1993 (2013) doi:10.1242/dev.087908


# The secreted *AdamTS-A* metalloprotease is required for collective cell migration

**Afshan Ismat, Alan M. Cheshire and Deborah J. Andrew***

## SUMMARY

Members of the ADAMTS family of secreted metalloproteases play crucial roles in modulating the extracellular matrix (ECM) in development and disease. Here, we show that ADAMTS-A, the *Drosophila* ortholog of human ADAMTS 9 and ADAMTS 20, and of *C. elegans* GON-1, is required for cell migration during embryogenesis. *AdamTS-A* is expressed in multiple migratory cell types, including hemocytes, caudal visceral mesoderm (CVM), the visceral branch of the trachea (VBs) and the secretory portion of the salivary gland (SG). Loss of *AdamTS-A* causes defects in germ cell, CVM and VB migration and, depending on the tissue, *AdamTS-A* functions both autonomously and non-autonomously. In the highly polarized collective of the SG epithelium, loss of *AdamTS-A* causes apical surface irregularities and cell elongation defects. We provide evidence that ADAMTS-A is secreted into the SG lumen where it functions to release cells from the apical ECM, consistent with the defects observed in *AdamTS-A* mutant SGs. We show that loss of the apically localized protocadherin *Cad99C* rescues the SG defects, suggesting that Cad99C serves as a link between the SG apical membrane and the secreted apical ECM component(s) cleaved by ADAMTS-A. Our analysis of *AdamTS-A* function in the SG suggests a novel role for ADAMTS proteins in detaching cells from the apical ECM, facilitating tube elongation during collective cell migration.

**KEY WORDS: ADAMTS, Collective migration, *Drosophila*, GON-1, Salivary gland**

## INTRODUCTION

Cell migration is crucial to shaping and positioning tissues during development, with some cells migrating extensive distances to populate various tissues. Cell migration also occurs throughout life, such as during tissue infiltration of immune cells, bone remodeling and wound healing. Tumor metastasis, the process by which tumor cells leave their site of origin to invade a secondary tissue, also requires cell migration. Cells move as individuals, as groups or as intact epithelia. Parts of cells also migrate, as observed with the axonal projections of neurons or fine branches of *Drosophila* tracheoles.

Several complex and delicately orchestrated events underlie directed cell movement (Alberts et al., 2002). Migrating cells extend actin-rich cytoplasmic protrusions (filopodia, lamellipodia and pseudopodia) in the direction of migration. Such protrusions form by actin polymerization at the leading edge, which pushes the cell membrane forwards. Polymerization of the actin filament plus ends enriched near the leading edge is counteracted by depolymerization of the actin filament minus ends deeper in the cell. For cells to move, they must also attach to a substratum. Attachment is mediated by integrins, which are transmembrane heterodimeric signaling molecules that recognize and bind components of the extracellular matrix (ECM), such as collagen and fibronectin, and that also bind proteins within the cell that are linked to the actin cytoskeleton (Ginsberg et al., 1992; Schwartz, 1992; Sastry and Horowitz, 1993). With force provided by myosins, a cell contracts to release the tension created by the cellular protrusions at the leading edge, bringing the bulk of the cell forward. The trailing edge must simultaneously release from the substratum to allow forward movement.

Department of Cell Biology, The Johns Hopkins University School of Medicine, 725 North Wolfe Street, Baltimore, MD 21205-2196, USA.

*Author for correspondence (dandrew@jhmi.edu)

**Accepted 25 February 2013**

Cells typically travel through and upon the ECM, a complex mixture of proteins and polysaccharides. The ECM, which is produced and secreted by cells, fills the intercellular space to help determine the shape and mechanical properties of many tissues. The complex fibrillar meshwork of the ECM, once thought to primarily provide structural support and tissue integrity, plays an active role in regulating cell behavior (Rozario and DeSimone, 2010; Brown, 2011; Wolf and Friedl, 2011). ECM proteoglycans sequester and modulate chemical signals, including growth factors and guidance molecules. Importantly, adhesions between cells and the ECM are crucial determinants of the rates and directions of cell movement, with tight adhesions correlating with slower movement and weaker adhesions correlating with more rapid movement. Consequently, too little or too much adhesion can prevent movement entirely (Gullberg and Ekblom, 1995; Streuli, 1999).

Much is known about single cell migration and interactions between the cell and ECM. Much less is known about collective cell migration. In single cell migration, the entire cell contacts the ECM, attaching and detaching from it as the cell moves forward. By contrast, during collective cell migration, cells contact both the ECM and other cells within the collective. Maintaining cell-cell adhesions while adjusting cell-ECM adhesions adds significant complexity to the process. Nonetheless, during both development and tumor metastasis, many cells migrate as collectives, moving as highly polarized epithelial sheets or branches, or as less polarized cell clusters or streams (Rørth, 2009).

Modulation of the ECM, which is crucial to both single cell and collective migration, is mediated by matrix metalloproteases (MMPs), a group of zinc-dependent proteases that regulates ECM composition, organization and function through cleavage of ECM components (Vu and Werb, 2000). MMPs are either secreted or membrane bound, either through a single transmembrane domain or covalently attached membrane anchor. ADAMTS metalloproteases (a disintegrin and metalloprotease with thrombospondin motifs), a subgroup of secreted zinc metalloproteases, have several domains that are distinct from those of classical MMPs (Blelloch and Kimble, 1999; Nishiwaki et

al., 2000; Apte, 2004). Based on studies in *C. elegans*, ADAMTS metalloproteases are thought to clear a path in front of migrating cells to allow forward movement (Blelloch et al., 1999; Blelloch and Kimble, 1999; Nishiwaki et al., 2000).

The human genome encodes 19 ADAMTSs, many with redundant functions (Apte, 2004; McCulloch et al., 2009; Enomoto et al., 2010). Therefore, studies in *Drosophila*, which has only three ADAMTS proteins, can provide key insights into their mechanism of action. Here, we characterize *AdamTS-A* (currently known as CG14869), which is expressed in migratory populations, including cells that migrate as individuals and cells that migrate as highly polarized collectives. We show *AdamTS-A* is essential for migration of multiple tissues. Our studies of *AdamTS-A* function in the SG reveal that not only do ADAMTS proteins clear a path for migration, as suggested for *C. elegans* GON-1, but may also function in cell detachment.

## MATERIALS AND METHODS

### *Drosophila* strains

The Bloomington Stock Center (Indiana University, Bloomington, IN, USA) provided $if^{k27e}$ (Wilcox et al., 1989), $mew^{m6}$ (Brower et al., 1995), *tub*-GAL4, $Df(3R)Exel^{6174}$, *UAS-srcEGFP*, *UAS-TmemGFP* and $tud^{1}$ (Boswell and Mahowald, 1985). M. Frasch (Universität Erlangen-Nürnberg, Erlangen, Germany) provided $bHLH54F^{598}$ (Ismat et al., 2010), *5053A*-GAL4 and *croc-lacZ* (Häcker et al., 1995). R. Lehmann (Skirball Institute, New York, USA) provided *nos*-GAL4 (Van Doren et al., 1998). S. Hayashi (RIKEN CDB, Kobe, Japan) provided *btl*-GAL4 (HVII) (Shiga et al., 1996). N. Perrimon (Harvard University, Cambridge, MA, USA) provided $wb^{4Y18}$ (Martin et al., 1999). C. Dahmann (Max Planck Institute, Dresden, Germany) provided $Cad99C^{57A}$ and $Cad99C^{120B}$. Our lab generated $trh^{8}$ (Isaac and Andrew, 1996), *fkh*-GAL4 (Henderson and Andrew, 2000) and *sage*-GAL4 (Chung et al., 2009).

### Generation of the *AdamTS-A* knockout

The translation start site through the cysteine-rich domain of the *AdamTS-A* ORF was deleted by homologous recombination (Gong and Golic, 2003) and confirmed by PCR. *AdamTS-A* knockout lines failed to complement $Df(3R)88F5^{e03525\text{-}d01653}$ and $Df(3R)Exel^{6174}$, and failed to express detectable transcript. The $AdamTS\text{-}A^{KO}$ and deficiencies are maintained over the TM6B, Ubx-lacZ balancer, as both genotypes are lethal over TM3, which carries an *AdamTS-A* allele (Nelson and Szauter, 1992). Primers used to generate the knock out and other tools are described in supplementary material Table S1.

### Construction of UAS-AdamTS-A and UAS-AdamTS-A-GFP

Two versions of *UAS-AdamTS-A* and *UAS-AdamTS-A-GFP*, corresponding to the two ORFs predicted on Flybase, were generated by subcloning a cDNA into the Gateway vectors (http://emb.carnegiescience.edu/labs/murphy/Gateway%20vectors.html). Although transcripts were detected with both versions of UAS-*AdamTS-A*, protein was detected with only the shorter form, suggesting that only the smaller ORF is made. To generate an enzyme-dead version of ADAMTS-A, the glutamate at position 439 was mutated to an alanine using the QuickChange Site-Directed Mutagenesis Kit (Stratagene).

### Tissue-specific rescue experiments

All tissue-specific rescue experiments were performed with the $AdamTS\text{-}A^{KO}$ in trans to $Df(3R)88F5^{e03525\text{-}d01653}$. All fly lines were balanced over *lacZ* balancers and stained with βGalactosidase (βGal) to distinguish homozygotes.

### Transmission electron microscopy (TEM)

TEM analysis was performed on stage 11-12 $AdamTS\text{-}A^{KO}$ and wild-type (Canton S) embryos as previously described (Myat and Andrew, 2000). $AdamTS\text{-}A^{KO}$ homozygotes were selected prior to fixation by the absence of GFP using *UAS-srcEGFP/UAS-srcEGFP; AdamTS-*$A^{KO}$*/TM6B, twi*-GAL4.

### Staining procedures

Immunohistochemistry and *in situ* hybridization were performed as described previously (Reuter and Scott, 1990; Azpiazu and Frasch, 1993; Knirr et al., 1999). Rabbit polyclonal antibodies used: anti-Vasa (1:200, Santa Cruz Biotechnology), anti-βgal (1:3000, Capell), anti-GFP (1:10,000, Molecular Probes), anti-GM130 (1:100, Abcam), anti-Rab11 [1:500 (Satoh et al., 2005); R. Cohen, University of Kansas, Lawrence, KS, USA], anti-Vps16 (1:100, H. Kramer, University of Texas Southwestern Medical Center, Dallas, TX, USA), anti-Cad99C (1:10,000; C. Dahmann, Max Planck Institute, Dresden, Germany), anti-CC3 [1:100, Cell Signaling, anti-SAS (1:500, unpublished)]. Rat polyclonal anti-SG1 (1:10,000) (Abrams et al., 2006) and rat anti-ADAMTS-A (1:500, our lab) were used. Mouse monoclonal antibodies used were: anti-2A12 [1:10, Developmental Studies Hybridoma Bank (DSHB)], anti-Crb (Cq4) (1:100-DAB, 1:10-fluorescence, DSHB), anti-α-spectrin (1:2, DSHB), anti-βgal (1:5000-DAB, 1:500-fluorescence, Promega), anti-GFP (1:200, Molecular Probes), anti-actin (1:2000, MP Biochemicals), anti-CSP2 (1:40, DSHB) and anti-FasIII (1:100, DSHB). Secondary biotinylated anti-mouse, biotinylated anti-rabbit, biotinylated anti-rat, goat anti-mouse-555, goat anti-rat488, goat anti-rabbit488 and goat anti-rat568 were used.

Rat antiserum to ADAMTS-A was generated against inclusion body preparations of *E. coli* expressing residues 298-469 of the *AdamTS-A* ORF. The antiserum does not detect endogenous levels of ADAMTS-A protein, but does detect overexpressed protein.

### Salivary gland cell length measurements

Stage 12 wild-type, $AdamTS\text{-}A^{KO}$ and $AdamTS\text{-}A^{KO}$ $Cad99C^{57A/120B}$ embryos were stained using antibodies against SAS (apical membrane) and α-spectrin (basolateral membrane), and 0.5 μm sections imaged on a Zeiss LSM 510-Meta confocal microscope with a 100× objective. The lengths of the three distalmost cells were measured from the center of the apical surface to the center of the basal surface using ImageJ software and converted from pixels to μm.

### Western blot analysis

Wild-type (Canton S), $AdamTS\text{-}A^{KO}$, *tub*-GAL4::UAS-*AdamTS-A* and *tub*-GAL4::UAS-$AdamTS\text{-}A^{E439A}$ embryos were dechorionated and sorted for absence of GFP on an embryo sorter (Union Biometrica). Approximately 50 μl of embryos were resuspended in 200 μl sample buffer [Tris-HCl (pH 6.8), SDS, bromophenol blue, glycerol, β-mercaptoethanol]. Samples (20 μl each) were run on 6% SDS-PAGE gels, transferred to methanol-treated PVDF membrane and exposed to Kodak film using enhanced chemiluminescence (ECL) reagents (GE-Healthcare). Primary antibodies used were: anti-Cad99C (1:10,000) (D'Alterio et al., 2005) (D. Godt, University of Toronto, Canada) and anti-βtubulin (E7) (1:1000, DSHB). HRP-conjugated secondary antibodies were used at 1:10,000.

## RESULTS

### *AdamTS-A* is expressed in several migratory tissues

Mammalian ADAMTS family members are expressed in a variety of tissues, and are important for a wide range of developmental and disease processes (Vázquez et al., 1999; Sandy et al., 2001; Jönsson-Rylander et al., 2005; Dunn et al., 2006; Held-Feindt et al., 2006; Murphy, 2008; McCulloch et al., 2009; Enomoto et al., 2010; Kessenbrock et al., 2010). Human ADAMTS genes have been grouped into four major subfamilies based on sequence and functional similarities (Fig. 1A) (Brocker et al., 2009). Family A includes ADAMTS 9 and ADAMTS 20, which cleave aggrecan, versican and brevican (Sandy et al., 2001; Apte, 2004; Nakada et al., 2005; Held-Feindt et al., 2006; Silver et al., 2008; McCulloch et al., 2009). Family B, the largest subgroup, includes ADAMTS 7 and ADAMTS 12, which cleave cartilage oligomeric matrix protein (COMP) (El-Hour et al., 2010). Family C – ADAMTS 2, ADAMTS 3 and ADAMTS 14 – processes procollagen types I-III (Abbaszade et al., 1999; Apte, 2004; Jones and Riley, 2005). ADAMTS 13, the

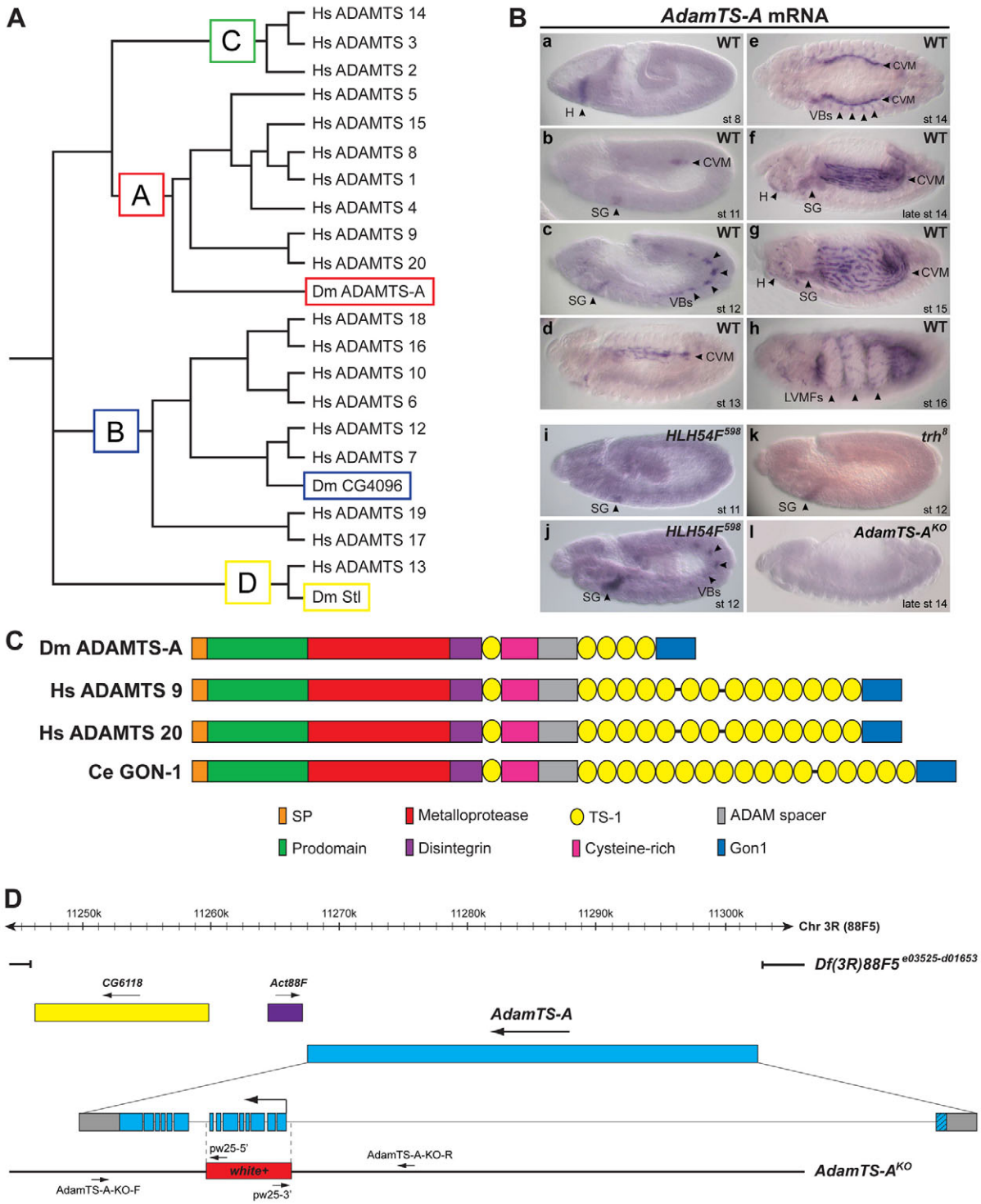


**Fig. 1. *AdamTS-A* encodes an ADAMTS metalloprotease expressed in migratory tissues.** (**A**) Rooted phylogenetic tree of human and *D. melanogaster* ADAMTS proteins separated into four major groups (A-D). (**B**) *AdamTS-A* mRNA is expressed in hemocytes (H) (a,f,g), caudal visceral mesoderm (CVM (b,d-g), salivary gland (SG) (b,c,f,g), tracheal visceral branch (VBs) (c,e) and longitudinal visceral muscle fibers (LVMFs) that form from CVM (h). *AdamTS-A* mRNA expression is absent in the posterior regions (presumed CVM) at stage 11 (i) and stage 12 (j) of $HLH54F^{598}$ embryos, even when the staining is overdeveloped. *AdamTS-A* mRNA is absent in the region of the VBs in a $trh^{8}$ embryo (k). *AdamTS-A* mRNA expression is absent in $AdamTS\text{-}A^{KO}$ embryos (l). Images are lateral views with anterior towards the left, with the exception of e, which shows a dorsal-ventral view, anterior towards the left. (**C**) Protein domain comparisons of *Drosophila* (Dm) ADAMTS-A, human (Hs) ADAMTS 9, Hs ADAMTS 20 and *C. elegans* (Ce) GON-1, showing conserved domains: signal peptide (SP), prodomain, metalloprotease, disintegrin, thrombospondin-like 1 repeat (TS-1), cysteine-rich, ADAM spacer and Gon1 domain. (**D**) *AdamTS-A* maps to cytological region 88F5 and has 14 exons, with a translation start in exon 2 and a translation stop in exon 14. $Df(3R)88F5^{e03525\text{-}d01653}$ removes three genes, *CG6118, Act88F* and *AdamTS-A* (also known as *CG14869*). The region removed in the $AdamTS\text{-}A^{KO}$ and replaced with the $white^{+}$ gene is shown. Primer pairs *AdamTS-A*-KO-F, pw25-5′ and *AdamTS-A*-KO-R, pw25-3′ were used to confirm homologous recombination (see supplementary material Table S1).

single Family D member, cleaves von Willebrand factor (Dong et al., 2002). The *Drosophila* genome encodes three ADAMTS proteins, two of which are completely uncharacterized (Fig. 1A). *stall* (*stl*), which is most similar to ADAMTS 13 of the D group, functions in ovarian follicle cell formation (Ozdowski et al., 2009), whereas the uncharacterized *CG4096* gene is most similar to the ADAMTS B group. Here, we focus on the previously uncharacterized ADAMTS-A, the single *Drosophila* A group ADAMTS (supplementary material Fig. S1).

ADAMTS secreted proteases contain several domains, many with undetermined functions. All contain an N-terminal signal peptide (SP), a prodomain, a metalloprotease domain, a disintegrin domain, thrombospondin-type I (TS-1) repeats and a cysteine-rich domain (Fig. 1C). *Drosophila* ADAMTS-A, human ADAMTS 9 and ADAMTS 20, and *C. elegans* GON-1 contain an additional C-terminal cysteine-rich Gon1 domain (Fig. 1C; supplementary material Fig. S1) (Llamazares et al., 2003; Somerville et al., 2003).

*AdamTS-A* is expressed in hemocytes (H) and caudal visceral mesoderm (CVM), cells that migrate as individuals (Fig. 1Ba,b,d-g). The CVM is a population of mesoderm cells that migrates anteriorly, spreads dorsally and later forms the outer layer of longitudinal visceral muscle fibers (LVMF) (Fig. 1Bb,d-h). The visceral branch (VB) of the trachea migrates as part of a polarized collective of cells and expresses *AdamTS-A* during mid-embryogenesis (Fig. 1Bc,e). The salivary gland (SG), which migrates as a fully intact and highly polarized collective, expresses *AdamTS-A* in the secretory cells from invagination at stage 11 to the end of migration (Fig. 1Bb-h). Expression of *AdamTS-A* in the early CVM and tracheal VB was

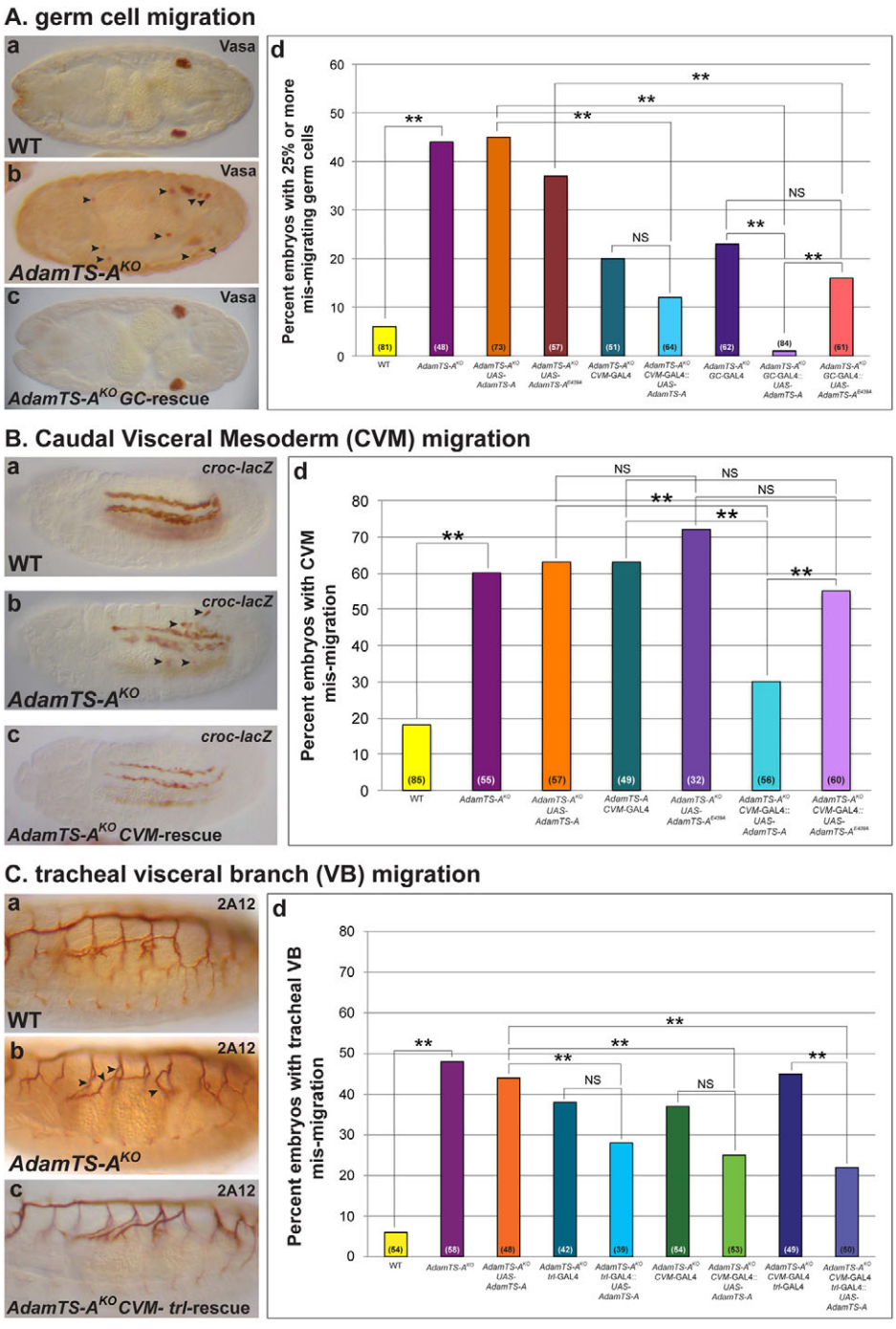


**Fig. 2. Loss of *AdamTS-A* causes migration defects.** (**A**) Germ cells (GCs) mis-migrate in *AdamTS-A* mutants. (a) Wild-type stage 16 embryo stained with anti-Vasa shows GCs coalesced in two tight clusters on either side the embryo. (b) *AdamTS-A*$^{KO}$ embryo has many mis-migrating GCs (black arrowheads). (c,d) Expressing *AdamTS-A* in only the GCs completely rescues migration. All embryos are dorsal-ventral views with anterior towards the left. (d) Quantification of the percentage total stage 15-17 embryos displaying 25% or more mis-migrating GCs in wild type, *AdamTS-A*$^{KO}$, rescue and controls. (**B**) Caudal visceral mesoderm (CVM) cells mis-migrate in *AdamTS-A* mutants. (a) Lateral view of a stage 14 wild-type embryo expressing the *croc-lacZ* reporter that marks CVM cells. (b) *AdamTS-A*$^{KO}$ embryo has many mis-migrating CVM cells (black arrowheads). (c,d) Expressing *AdamTS-A* in the CVM rescues the CVM migration defect. (d) Quantification of the percentage total stage 13-14 embryos displaying mis-migrating CVM cells in wild type, *AdamTS-A*$^{KO}$, rescue and controls. (**C**) Tracheal visceral branches (VBs) mis-migrate in *AdamTS-A* mutants. (a) Lateral view of a stage 16 wild-type embryo stained with anti-2A12 to mark the tracheal lumen. VBs 3-6 were analyzed. (b) *AdamTS-A*$^{KO}$ embryo displays mis-migrating VBs (black arrowheads). (c,d) Expressing *AdamTS-A* in both trachea and CVM provides the best rescue of VB migration. (d) Quantification of the percentage total stage 15-16 embryos displaying mis-migrating tracheal VBs in wild type, *AdamTS-A*$^{KO}$, rescue and controls. All quantifications were with *AdamTS-A*$^{KO}$ in *trans* to *Df(3R)88F5*. All embryos in B,C are lateral views with anterior towards the left. Rescue experiments were carried out at 25°C. GAL4 lines used: *germ cell*-GAL4 (*GC*-GAL4): *nanos*-GAL4, *CVM*-GAL4: *5053A*-GAL4, and *tracheal*-GAL4 (*trl*-GAL4): *btl*-GAL4 (II). Number of embryos scored for each genotype is in parentheses. $^{**}P<0.05$ based on a G-test of statistical independence. NS, not statistically significant.

confirmed using mutations in the transcription factor genes *HLH54F* and *trh*, which are required for gene expression in each respective cell type (Fig. 1Bi-k) (Ismat et al., 2010; Chung et al., 2011). Thus, *AdamTS-A* is expressed in four distinct migratory tissues: hemocytes, CVM/LVMF, tracheal VB and SG.

## Loss of *AdamTS-A* affects several distinct migratory cell types

To analyze *AdamTS*-A function, we created a small deficiency, *Df(3R)88F*, that removes *AdamTS-A* and two neighboring genes, and we created a knockout allele, *AdamTS-A$^{KO}$* (Fig. 1D; see Materials and methods). The *AdamTS-A$^{KO}$* allele is RNA null (Fig. 1Bl), and lethal over deficiencies that remove *AdamTS-A* (supplementary material Table S2). We first examined the effects of *AdamTS-A* loss in a well-characterized migratory population, the germ cells (GC). Prior to migration, GCs are encapsulated into the pocket of the posterior midgut primordium (supplementary material Fig. S2A, Fig. S3A). GCs then cross the posterior midgut epithelium and migrate to the somatic gonad (supplementary material Fig. S2B-E, Fig. S3B,C). By late embryogenesis, most GCs are found in two tight clusters, one on either side of the embryo (Fig. 2Aa; supplementary material Fig. S2F, Fig. S3D) (Starz-Gaiano and Montell, 2004; Kunwar et al., 2006). We found ~6% of late stage wild-type embryos had 25% or more GCs outside the clusters (Fig. 2Aa,d). By contrast, ~45% of *AdamTS-A$^{KO}$/Df(3R)88F5* embryos (hereafter referred to as *AdamTS-A$^{KO}$*) had 25% or more of their GCs outside the clusters (Fig. 2Ab,d). GCs do not detectably express *AdamTS-A*, but migrate in close apposition to the CVM, which does (Fig. 1Bb,d-g; supplementary material Fig. S2), suggesting that ADAMTS-A secreted from the CVM could affect GC migration. Interestingly, expressing wild-type *AdamTS-A* in only the GCs completely rescued the GC migration defect relative to wild type, and to the *GC*-GAL4 and *UAS-AdamTS-A* controls (Fig. 2Ac,d; compare bar 8 and bars 1, 3 and 7, supplementary material Fig. S3A-E′). Expressing wild-type *AdamTS-A* just in the CVM reduced the GC migration defect compared with control animals (bar 6), but only significantly when compared with the *UAS-AdamTS-A* (bar 3), and not *CVM*-GAL4 (bar 5) controls (Fig. 2Ad; supplementary material Fig. S3F-J‴). These results suggest ADAMTS-A works better for GC migration when expressed tissue autonomously, although it is presumably normally provided non-autonomously by the CVM (based on *AdamTS-A* mRNA expression). To determine whether protease activity is required, we tested an enzyme-dead version, which did not rescue GC migration as well as the wild-type protein did (Fig. 2Ad, bar 9).

CVM cells migrate in two rows in a posterior to anterior direction along the length of the embryo, as shown with *croc-lacZ*, a CVM marker (Fig. 2Ba; supplementary material Fig. S2, Fig. S3F-J‴) (Häcker et al., 1995). In *AdamTS-A* mutants, many CVM cells migrate away from these two rows, with a greater than 40% increase in the number of embryos displaying mis-migrating CVM cells (Fig. 2Bb,d). Confocal imaging of the CVM revealed an even more severe phenotype than suggested by the HRP-stained samples (supplementary material Fig. S4, arrowheads) (Fig. 2Ba-d). As anticipated, expressing *AdamTS-A* just in the CVM significantly rescued the migration defect (Fig. 2Bc,d, bar 6; supplementary material Fig. S3J-J‴), signifying a tissue-autonomous function for

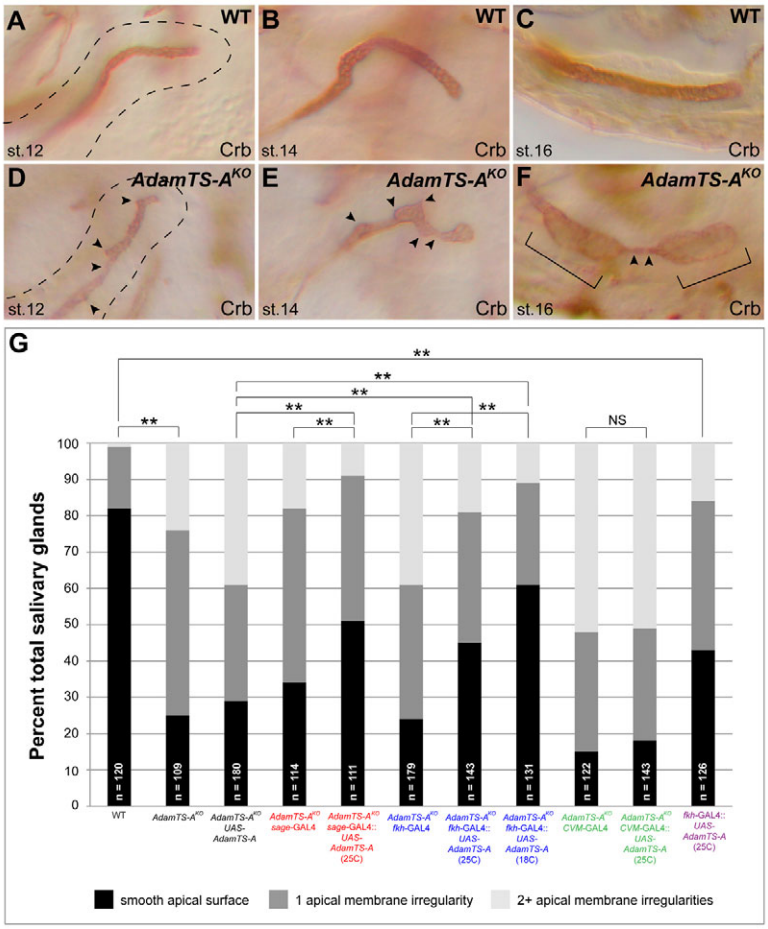


**Fig. 3. Loss of *AdamTS-A* causes SG apical irregularities.** (**A-F**) Wild-type (A-C) and *AdamTS-A$^{KO}$* (D-F) embryos were immunostained with anti-Crb, an apical membrane marker. The basal membrane of the SG is outlined in black (A,D). In wild type, the apical surface of the SG is smooth with a uniform diameter throughout its length (A-C). At stage 12 and 14 (D,E), the apical surface of the *AdamTS-A$^{KO}$* is rough and jagged with an irregular diameter (black arrowheads). At stage 16 (F), the apical surface displays constrictions (black arrowheads) and bulges (brackets). SGs in A,B,D,E are lateral views. SGs in C and F are ventral views. (**G**) Quantification of the percentage of total SGs displaying a smooth apical surface, one apical irregularity, or two or more apical irregularities. Number of SGs scored for each genotype is shown in each bar. ***P*<0.05 based on a G-test of statistical independence. NS, not statistically significant.

ADAMTS-A in the CVM. Here, also, the enzyme-dead version of ADAMTS-A did not rescue the migration defect (Fig. 2Bd, bar 7), indicating that metalloprotease activity is required for function.

In *AdamTS-A* mutants, the tracheal VBs (3-6) mis-migrated with a 40% increase compared with wild type (Fig. 2Ca,b). We expected tracheal expression of *AdamTS-A* might rescue the VB migration defects; however, as *AdamTS-A* is also expressed in the CVM cells upon which the VBs migrate (supplementary material Fig. S5) (Boube et al., 2001), expressing *AdamTS-A* just in the CVM might also rescue VB migration. Expressing *AdamTS-A* in either the trachea or the CVM alone reduced the VB mis-migration defect compared with controls, although only significantly when compared with the *UAS-AdamTS-A* control (Fig. 2Cd, compare bar 5 and 3, 4, compare bar 7 and 3, 6; supplementary material Fig. S3F-I,K-N). Simultaneous expression of *AdamTS-A* in the trachea and CVM significantly rescued VB migration relative to all controls (Fig. 2Cd, compare bar 9 and 3, 8; supplementary material Fig. S3F-I,K-N). Although expression in both tissues provides the best rescue of tracheal migration, we do not know whether expression in the CVM contributes directly by providing ADAMTS-A activity to the VBs, or indirectly by rescuing migration of the CVM cells upon which the VBs migrate. Altogether, the results from the GCs, CVM and tracheal VBs reveal that ADAMTS-A is required for migration of several cell types, including cells that migrate as individuals (GCs and CVM) and cells that migrate as part of an intact epithelium (VBs).

## *AdamTS-A* mutant salivary glands have apical irregularities

To determine how ADAMTS-A functions in collective cell migration, we turned to the embryonic SGs, which express *AdamTS-A* prior to and during posterior migration. SGs form from two plates of ~100 polarized epithelial cells each on the ventral surface of parasegment two. Through coordinated cell shape changes, cell rearrangement, growth and migration, the SG primordia form fully internalized and elongated tubes. Neither cell death nor cell division normally occurs during SG development, and, during the entire process, the SG remains fully polarized (Fig. S3V-Y) (Kerman et al., 2006; Maruyama and Andrew, 2012). The basal surfaces of SG cells form the outside of the tube, exhibiting extensive lamellipodial protrusions during migration (Cheshire et al., 2008). The apical surfaces form the inner lining of the tube, directly contacting the developing matrix-filled lumen. Based on previous work suggesting that matrix metalloproteases function to clear a path for migration, we expected defects similar to those observed with integrin mutants, in which the SGs completely fail to migrate and eventually buckle, forming U-shaped tubular structures (Fig. 4F,H,J) (Bradley et al., 2003). We did not observe integrin-like phenotypes with *AdamTS-A* loss; instead, we observed apical surface defects. Wild-type SGs displayed apical surfaces that were smooth and uniform in diameter at all stages (Fig. 3A-C,G), whereas *AdamTS-A$^{KO}$* SGs had multiple deformations, including rough irregular surfaces at early stages (Fig. 3D,E,G), and constrictions

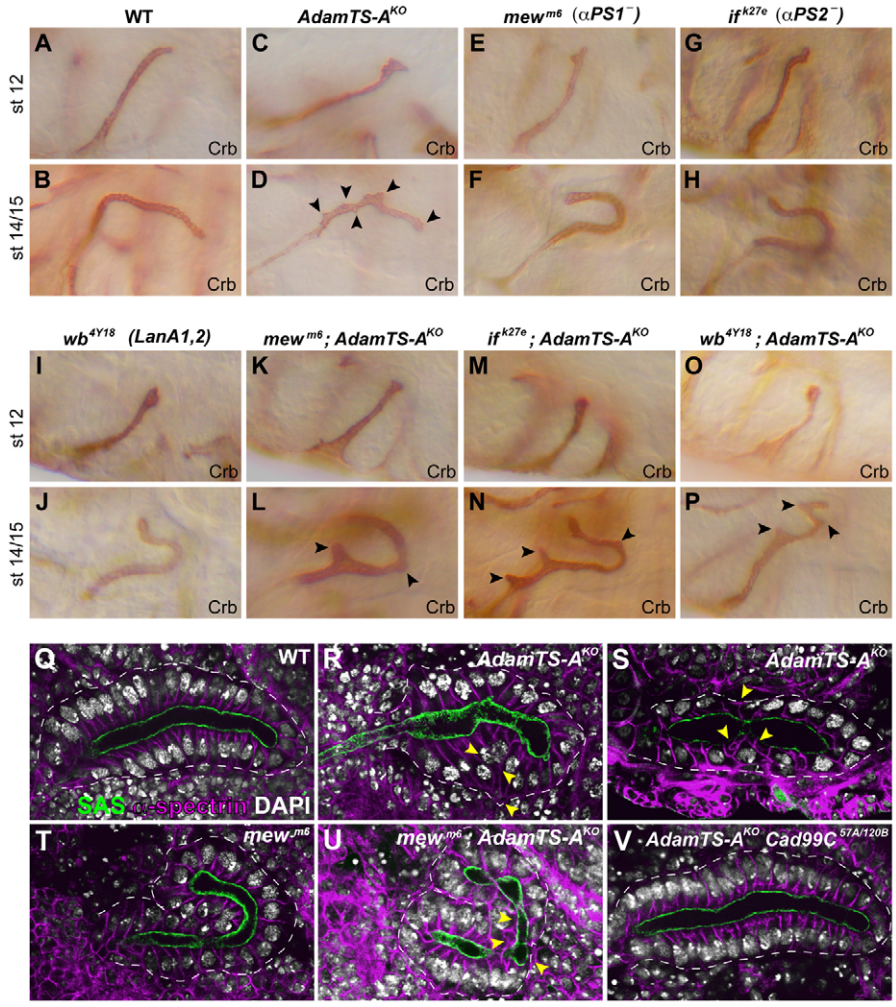


**Fig. 4. The apical defect in *AdamTS-A$^{KO}$* does not depend on SG migration.** (**A**) Stage 12 wild-type SG stained using antibodies against Crb has a smooth apical surface prior to posterior migration (left to right in all panels). (**B**) Stage 14/15 wild-type SG at a later stage. (**C**) Stage 12 *AdamTS-A$^{KO}$* SG shows apical irregularities. (**D**) Stage 14 *AdamTS-A$^{KO}$* SG has a rough and irregular apical surface (black arrowheads). (**E-J**) Integrin pathway mutants *mew$^{m6}$* (α*PS1* null) (E,F), *if$^{k27e}$* (α*PS2* null) (G,H) and *wb$^{4Y18}$* (*LanA1,2* null) (I,J) show similar phenotypes to *AdamTS-A$^{KO}$* at stage 12 (compare E,G,I with C). At stage 14/15, *mew$^{m6}$* (F), *if$^{k27e}$* (H) and *wb$^{4Y18}$* (J) SGs look completely different from the *AdamTS-A$^{KO}$* SG (D). (**K-P**) Removing the integrin pathway and *AdamTS-A* caused an additive phenotype. At stage 12, *mew$^{m6}$; AdamTS-A$^{KO}$* (K), *if$^{k27e}$; AdamTS-A$^{KO}$* (M) and *wb$^{4Y18}$; AdamTS-A$^{KO}$* (O) look similar to the *AdamTS-A$^{KO}$* (C) or the integrin pathway mutants alone (E,G,I). At stage 14/15, the SG tube was elongated and buckled, and had the irregular apical protrusions observed with loss of *AdamTS-A* (black arrowheads in L,N,P). (**Q-V**) Stage 15 SGs of wild type (Q), *AdamTS-A$^{KO}$* (R,S), *mew$^{m6}$* (T), *mew$^{m6}$; AdamTS-A$^{KO}$* double mutants (U) and *AdamTS-A$^{KO}$ Cad99C$^{57A/120B}$* double mutants stained with anti-SAS (green), anti-α-spectrin (magenta) and DAPI (white). Basal surfaces of SGs are outlined in white. Both wild type (Q) and integrin pathway mutants alone (T) display a regular array of nuclei around the lumen (green). Loss of *AdamTS-A* alone or *mew$^{m6}$; AdamTS-A$^{KO}$* resulted in an irregular arrangement of cells surrounding the lumen (yellow arrowheads in R,S,U). Removing Cad99C rescued the SG apical defect and regular arrangement of cells around the lumen (V).

and bulges at later stages (Fig. 3F,G). Rescue of *AdamTS-A* SGs was complicated by our finding that overexpression of *AdamTS-A* in otherwise wild-type SGs also resulted in apical irregularities, suggesting some dose sensitivity (Fig. 3G; supplementary material Fig. S3Q-T). Two GAL4 drivers (*fkh*-GAL4 and *sage*-GAL4) were used to express *AdamTS-A* in the SG (Fig. 3G; supplementary material Fig. S3Q-T,V-Y). The best rescue was achieved with either the *sage*-GAL4 driver at 25°C (Fig. 3G; supplementary material Fig. S3Q-T,V-Y) or the *fkh*-GAL4 driver at 18°C, in which GAL4 activity and, presumably, expression levels are lower (Fig. 3G) (Brand et al., 1994). As *AdamTS-A* is predicted to encode a secreted protease, and as the basal surface of the SG contacts the CVM during mid- to late migration of both tissues (supplementary material Fig. S6C-H), we also asked whether CVM-driven expression of *AdamTS-A* could rescue the *AdamTS-A*$^{KO}$ SG defects. CVM-driven expression of *AdamTS-A* (supplementary material Fig. S3F-I) did not rescue the SG mutant phenotypes relative to any control (Fig. 3G). We conclude that *AdamTS-A* functions tissue autonomously in the SG.

## The apical irregularities in *AdamTS-A*$^{KO}$ do not depend on SG migration

The defects associated with *AdamTS-A*$^{KO}$ are not due to apoptosis, based on anti-CC3 antibody staining where wild type and *AdamTS-A* mutants show only the apoptosis that normally occurs during embryogenesis (Fan and Bergmann, 2010) (supplementary material Fig. S7; data not shown). We have also ruled out changes in cell fate, based on staining with a range of tissue-specific markers: CrebA, Sage and SG1 for the SG; Trh, Tango and Knirps for the trachea; Vasa for the GCs; and *croc-lacZ* (βgal) for the CVM (supplementary material Figs S5-7; data not shown). Whereas the defects in the GCs, CVM and tracheal VBs are likely due to mis-migration (Fig. 2), the SG defects do not appear to be. To determine whether the *AdamTS-A* SG phenotypes depend on migration, we assayed SGs in which *AdamTS-A*, integrin function, or both, were disrupted. The SG expresses *αPS1* (*mew* – FlyBase) and invaginates dorsally until it reaches the visceral mesoderm (VM), which expresses *αPS2* (*if* – FlyBase). Upon VM contact, the SG normally turns and migrates posteriorly in close contact with the VM, which also expresses *LamininA1,2* (*wb* – FlyBase) (Bradley et al., 2003; Vining et al., 2005). At stage 12, when the distal region of the SG first contacts the VM, slight irregularities in the apical surface were observed in the distal SG in integrin pathway mutants *αPS1*, *αPS2* and *LamininA1,2*, similar to those seen in *AdamTS-A*$^{KO}$ SGs (Fig. 4C,E,G,I; Fig. 3D). As the SG tube continued to elongate, the failure of the SG to migrate in integrin pathway mutants resulted in buckling of the SG tube (Fig. 4F,H,J). At this stage, the SG apical surfaces in the integrin pathway mutants were relatively smooth and uniform in diameter, distinctly different from the SGs of *AdamTS-A* mutants (Fig. 4D; Fig. 3E). Removing both *AdamTS-A* and integrin pathway function resulted in the same buckling defects observed in integrin pathway mutants and the same apical irregularities observed in *AdamTS-A* mutants (Fig. 4L,N,P). Thus, the *AdamTS-A* phenotypes do not require cell migration. Instead,

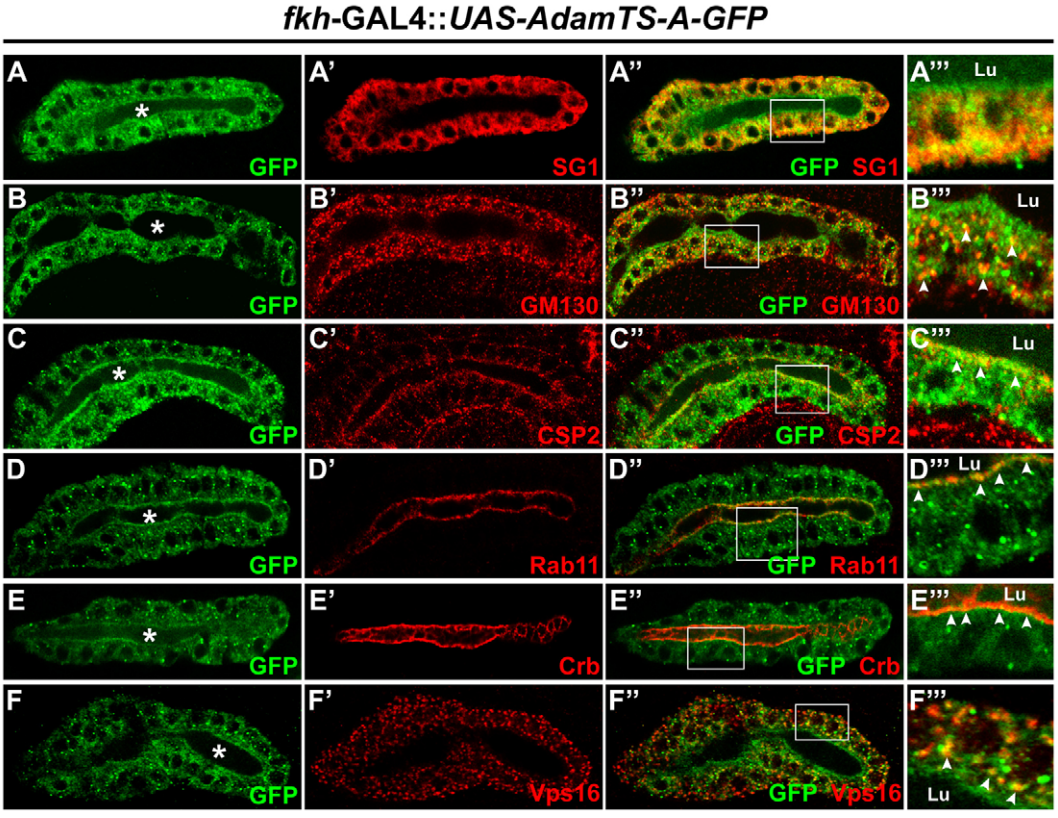


**Fig. 5. GFP-tagged ADAMTS-A is found in the apical region of the SG.** (**A-F‴**) *UAS-AdamTS-A-GFP* was expressed using *fkh*-GAL4 at 25°C. ADAMTS-A-GFP (GFP) (green) (A-F) colocalizes with the ER-specific α-Ph4αSG1 (red) (A′), the Golgi marker GM130 (red) (B′), the vesicle marker CSP2 (red) (C′) in secretory vesicles at/near the apical surface, the apical recycling endosome marker Rab11 (red) (D′), the apical marker Crb (red) (E′) and Vps16 (red) (F′), which is a marker of endocytic trafficking. (A‴-F‴) Enlargements of areas in the white boxes in A″-F″, with white arrowheads indicating colocalization. Very low levels of GFP are also detectable in the lumen (asterisks in A-F).

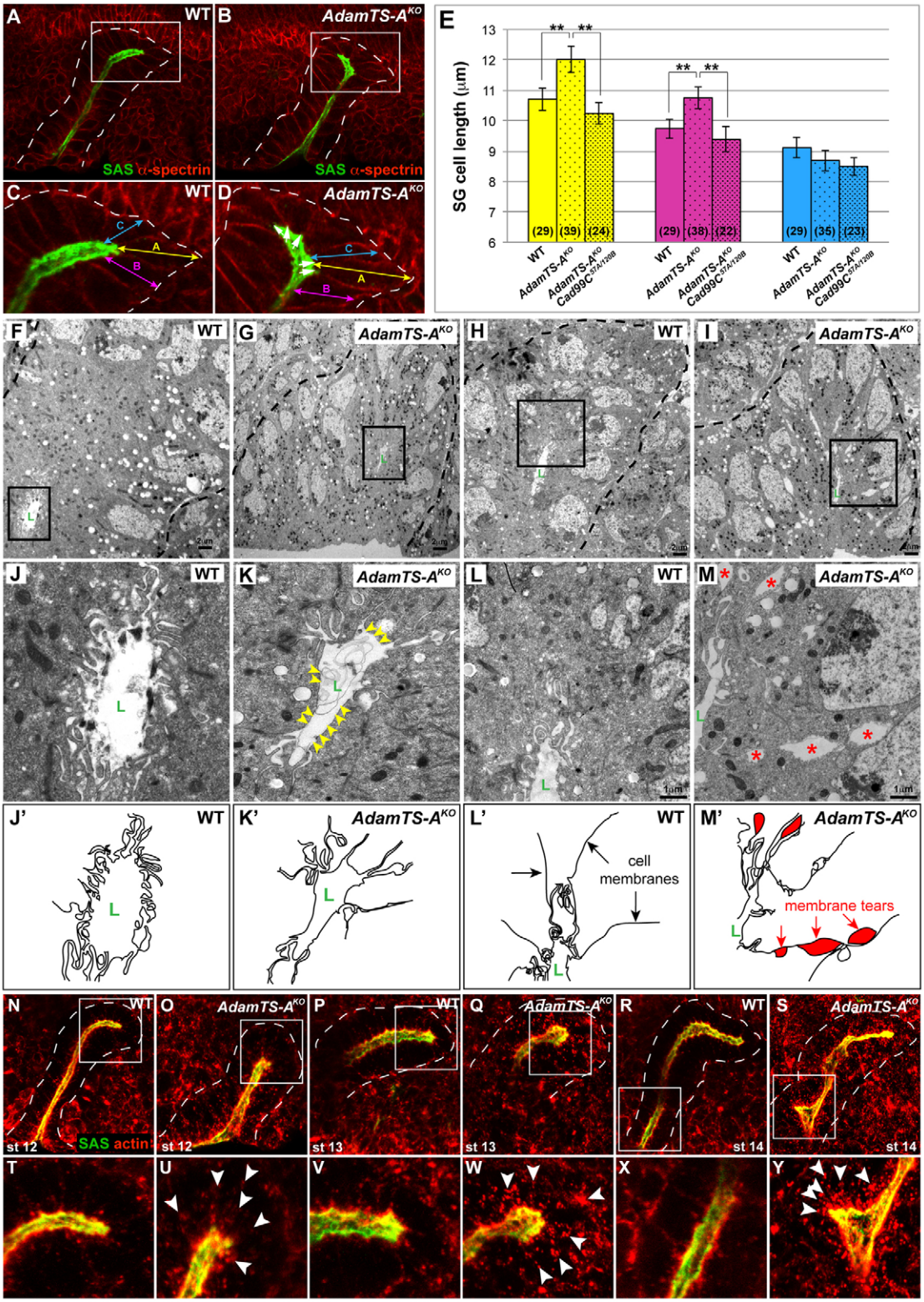


**Fig. 6.** See next page for legend.

we propose that the phenotypes associated with *AdamTS-A* loss are linked to the cell rearrangements required for tube elongation, a process largely unaffected by integrin loss (Bradley et al., 2003). Indeed, staining with DAPI (white) in combination with the apical marker SAS (green) and the basolateral marker α-spectrin (magenta) revealed irregularities in the arrangement of nuclei around the lumen in the *AdamTS-A*$^{KO}$ and *mew* (αPS1); *AdamTS-A* double mutants (Fig. 4R,S,U) compared with the regular array of nuclei in both wild type and *mew* mutant SGs (Fig. 4Q,T). Overall, this analysis suggests that *AdamTS-A* may normally facilitate the cell rearrangements that accompany SG tube elongation during posterior migration.

**Fig. 6. ADAMTS-A detaches SG cells from the apical extracellular matrix.** (**A-E**) Stage 12 wild-type (A,C) and *AdamTS-A*$^{KO}$ (B,D) embryos were stained using antibodies against SAS (apical membrane) (green) and α-spectrin (basolateral membrane) (red). The SG is outlined in white. (C,D) Enlargements of the distal-most cells of SGs in A,B; double arrows indicate the cells for which lengths were measured (cell A, yellow; cell B, pink; cell C, blue). In the *AdamTS-A*$^{KO}$, apical irregularities are between cells and are always associated with the cell membrane (white arrows in D). (E) Cell length measurements of the distal-most SG cells A, B and C from wild-type, *AdamTS-A*$^{KO}$ and *AdamTS-A*$^{KO}$ *Cad99C*$^{57A/120B}$ embryos. Number of cells measured is in parentheses. Data are expressed as mean±s.e.m. Statistical significance was determined at $^{**}P<0.05$ using Student's two-tailed *t*-test. (**F-M**) TEM images of stage 12 wild-type (F,H,J,L) and *AdamTS-A*$^{KO}$ (G,I,K,M) SGs. The distal-most region of the SG is outlined in black (F-I). (F,G,J,K) Low magnification (520×) TEM images of wild-type (F) and *AdamTS-A*$^{KO}$ (G) SGs show the lumen (green L) and surrounding SG cells. (J) High magnification (3800×) TEM image of boxed area in F. (K) High magnification (3800×) TEM image of boxed area in G shows a flatter apical surface (yellow arrowheads). (H,I,L,M) Low magnification (520×) TEM images of two different wild-type (H) and *AdamTS-A*$^{KO}$ (I) SGs show the lumen (L) and surrounding SG cells. (L) High magnification (2100×) TEM image of boxed area in H. (M) High magnification (2100×) TEM image of boxed area in I shows separations between cells (red asterisks). (**J′-M′**) Cartoon depictions of TEMs from J-M, respectively. (**N-Y**) Stage 12-14 wild-type (N,P,R,T,V,X) and *AdamTS-A*$^{KO}$ (O,Q,S,U,W,Y) embryos stained using antibodies against SAS (green) and α-actin (red). (T-Y) Enlargements of boxed regions from N-S show actin accumulation along the lateral regions (white arrowheads in U,W,Y) and at apical membrane irregularities (white arrowheads in Y). Actin levels in surrounding non-SG tissue are comparable in wild-type and *AdamTS*$^{KO}$ embryos (N-S).

## ADAMTS-A-GFP localizes to the apical surface of the SG

Our finding that loss of *AdamTS-A* may affect cell rearrangement during tube elongation raises the issue of where the protease is secreted. To localize ADAMTS-A, we generated and expressed a GFP-tagged version in the SG (Brand and Perrimon, 1993). ADAMTS-A-GFP was detected throughout SG cells, significantly overlapping the endoplasmic reticulum protein Ph4αSG1 (Fig. 5A-A‴), and the Golgi marker GM130 (Fig. 5B-B‴, arrowheads in B‴), indicating that ADAMTS-A is traveling through the secretory pathway. ADAMTS-A-GFP also overlaps with the secretory vesicle marker CSP2 only at the apical surface (Fig. 5C-C‴) and the apical recycling endosome marker Rab11 (Fig. 5D-D‴), suggesting ADAMTS-A is present in vesicles destined for apical secretion. ADAMTS-A-GFP was also enriched at the apical region where the apical membrane protein Crb is found (Fig. 5E-E‴). Finally, very low levels of ADAMTS-A-GFP were detected in the SG lumen (Fig. 5A-F). ADAMTS-A-GFP also overlapped with Vps16, a marker for endosome to lysosome trafficking (Fig. 5F-F‴), consistent with data showing that the level of ADAMTS-A is important for its proper function (Fig. 3G). Too much ADAMTS-A in the SG may result in targeting much of it for degradation. A similar staining pattern was observed with overexpression of an untagged version of ADAMTS-A, using an ADAMTS-A antibody that detects only overexpressed protein (supplementary material Fig. S3U-U‴). Overall, the staining pattern is consistent with ADAMTS-A travelling through the secretory pathway and being secreted apically.

## ADAMTS-A functions to detach SG cells from the apical ECM (aECM)

The apical surface of the SG contacts the lumen, which is filled with a fibrillar matrix first detectable during embryonic stage 11 (Myat and Andrew, 2002; Abrams et al., 2006). Thus, both the basal and apical surfaces of the SG contact an ECM. Staining SGs using antibodies against SAS, an apical membrane marker, and α-Spectrin, a basolateral marker, revealed that SG cells are fully polarized in *AdamTS-A* mutants and, just like wild type, migrate posteriorly (Fig. 6A-D). The staining also revealed that the apical irregularities in the *AdamTS-A*$^{KO}$ SGs localize between neighboring cells (Fig. 6D), supporting the idea that, although *AdamTS-A* mutant SGs extend in the right direction, the apical cell surfaces could be held back as the gland moves forward. To explore this idea further, we measured the lengths of the three distal-most SG cells (A, B and C) in wild-type and *AdamTS-A*$^{KO}$ embryos (yellow, pink and blue arrows in Fig. 6C,D, respectively). On average, two of the distal-most cells (cell A, cell B) of *AdamTS-A* mutant SGs were significantly longer than wild type (Fig. 6D,E), suggesting that the apical surfaces remain attached to the apical ECM as the basal surfaces extend posteriorly during migration. High magnification transmission electron microscopy (TEM) revealed two additional differences in *AdamTS-A* versus wild-type SGs: wild-type stage 12 SGs had highly convoluted apical surfaces, as previously observed (Myat and Andrew, 2002; Kerman et al., 2008) (Fig. 6J,J′), whereas *AdamTS-A* mutant SGs had smoother and flatter apical surfaces, perhaps suggesting a decrease in apical membrane turnover (Fig. 6K,K′). Wild-type SGs also had smooth, intact lateral cell membranes basal to the adherens junctions (Fig. 6L,L′), whereas some *AdamTS-A* mutant SGs showed separations along the lateral cell membranes, with the most extreme example showing significant separations at multiple sites (Fig. 6M,M′), suggesting increased tension between neighboring cells. Consistent with this idea, much higher levels of F-actin were observed at the apical surface and along the lateral surfaces of SG cells of *AdamTS-A*$^{KO}$ mutants compared with wild type (Fig. 6U,W). Very high levels of F-actin were also observed at the apical irregularities in later stage *AdamTS-A*$^{KO}$ glands (Fig. 6Y). Thus, the actin cytoskeleton appears to be under increased tension in *AdamTS-A* mutant SGs. Altogether, the apical separations between cells, the flatter apical surfaces and the increased actin levels in the *AdamTS-A*$^{KO}$ support a model in which ADAMTS-A functions to release the apical surfaces of SG cells from the apical matrix, allowing cells to more easily rearrange as the tube elongates and moves to its final position.

## *Cadherin99C* (*Cad99C*) loss suppresses the *AdamTS-A* mutant SG phenotype

We propose that ADAMTS-A functions to release SG cells from the apical ECM through cleavage of either apical ECM substrates or molecules that attach the apical membrane to the ECM. Either way, removal of a link between the apical membrane and apical ECM should reduce SG attachment and allow for fluid forward movement. The atypical cadherin Cad99C localizes to the apical surface of the developing SG, making it an ideal candidate for mediating this attachment (supplementary material Fig. S8B-B″) (S.-Y. Chung and D.J.A., unpublished). Indeed, removing *Cad99C* resulted in a significant rescue of the SG defects in the *AdamTS-A* mutants (compare Fig. 7C with 7B,D; Fig. 6E; compare Fig. 4V with 4R,S). To determine whether Cad99C is itself an ADAMTS-A substrate, we examined Cad99C levels in *AdamTS-A* mutant SGs, but found no differences compared with wild type (supplementary material Fig. S8B-C″). We then asked whether overexpression of ADAMTS-A in embryos would result in decreased Cad99C levels. Neither overexpression nor loss of *AdamTS-A* affected Cad99C levels (Fig. 7E), indicating that Cad99C is unlikely to be a direct substrate of ADAMTS-A. These results suggest a model in which Cad99C

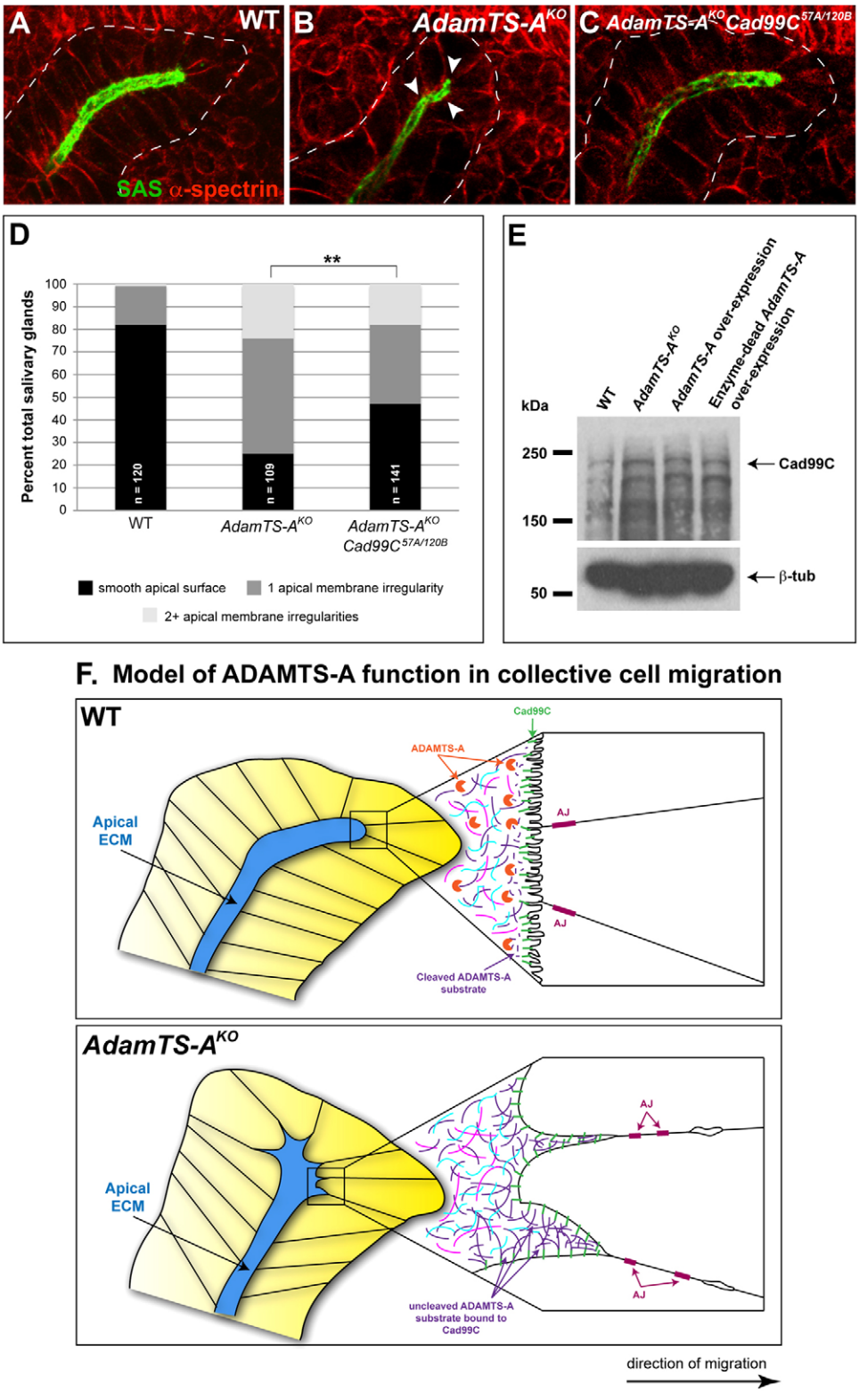


**Fig. 7. Loss of the protocadherin Cad99C rescues the *AdamTS-A* SG defects.** (**A-C**) Stage 12 wild-type (A), *AdamTS-A*$^{KO}$ (B) and *AdamTS-A*$^{KO}$ *Cad99C*$^{57A/120B}$ (C) SGs were stained using antibodies against SAS (green) and α-spectrin (red). The *AdamTS-A*$^{KO}$ *Cad99C*$^{57A/120B}$ double mutant (C) is similar to wild type, and unlike the *AdamTS-A* mutant (white arrowheads in B). SG basal surfaces are outlined in white. (**D**) Quantification of percentage total SGs displaying a smooth apical surface, one apical irregularity, or two or more irregularities. Removal of *Cad99C* (*Cad99C*$^{57A/120B}$) rescues the apical defect in the *AdamTS-A*$^{KO}$ SGs. (**$P<0.05$ based on a G-test for statistical independence). (**E**) Western blot reveals the same levels of Cad99C in wild-type embryos, embryos overexpressing either wild type or an enzyme-dead version of ADAMTS-A (*AdamTS-A*$^{E439A}$) and *AdamTS-A*$^{KO}$ embryos. Anti-β-tubulin antibody was the loading control. (**F**) A model of ADAMTS-A function. Cartoons depict the distal-most region of wild-type and *AdamTS-A*$^{KO}$ SGs. In wild type, the apical surface is convoluted where Cad99C is localized and presumably bound to ECM proteins. ADAMTS-A is proposed to cleave an unidentified secreted ECM component that binds Cad99C, allowing detachment of the apical surface during cell rearrangement. In the *AdamTS-A*$^{KO}$, the ECM component normally cleaved by ADAMTS-A remains bound to Cad99C, causing the apical surface to remain attached to the apical ECM. During the cell rearrangements of elongation, the apical membrane is pulled, often resulting in displacement of adherens junctions (AJs) deeper into the regions between neighboring cells and in cell separation.

links the apical membrane of SG cells to the apical ECM, and that Cad99C binds an ECM component normally cleaved by ADAMTS-A during the cell rearrangements of tube elongation (Fig. 7F).

## DISCUSSION

Here, we report the characterization of the *Drosophila* ADAMTS secreted metalloprotease ADAMTS-A. *AdamTS-A* is expressed in several migratory cell types during embryogenesis and its loss results in migration defects. ADAMTS-A appears to function both in the cells in which it is expressed, and in neighboring cells. In the highly polarized epithelial cells of the migrating SG, loss of *AdamTS-A* results in apical membrane irregularities that are linked to defects in the arrangement of SG cells around the central lumen. The distal-most cells of the migrating SG are over-elongated, and

there is increased tension between SG cells, and between SG cells and the apical surface. We show that ADAMTS-A travels through the secretory pathway and co-localizes with the apical recycling endosomal marker protein Rab11, and with only the apical pools of the general secretory vesicle marker CSP. Based on these findings, we propose that *AdamTS-A* functions to release the apical cell surface of individual SG cells from the underlying apical ECM, facilitating the cell rearrangements required for tube elongation during collective migration.

The SG migrates as a polarized collective, which, like a single migrating cell, has a leading edge that forms protrusions in the direction of migration, and a trailing edge that must detach from the substrate to allow forward movement. Contraction and migration of the proximal half of the gland allows the SG to detach from the ventral surface of the embryo and continue migrating posteriorly (Xu et al., 2008). Based on these observations, it has been suggested that the entire SG is comparable with a single migrating cell, with the distal region of the organ acting as the leading edge and the proximal region as the trailing edge. Collective cell migration involves not only the complex interplay between the entire collective and local environment, but also interactions among individual cells within the collective (Rørth, 2009). Interactions between the entire collective and environment include responses to guidance signals provided by surrounding cells, as well as formation and dissociation of adhesions between the migrating tissue and its extracellular environment. Within the collective, individual cells must coordinate their responses to guidance information by adjusting their shapes and position so that polarity is maintained throughout migration. Cells within the collective must also regulate both cell-cell and cell-matrix adhesions to allow coordinated movement relative to one another. Indeed, tube elongation requires SG cells to undergo 'convergence-extension', during which the cells must not only detach from one another but also from the apical ECM. Detachment of cells from one another depends on the turnover of E-cadherin (Pirraglia et al., 2010). We propose that detachment of SG cells from the apical matrix is facilitated by ADAMTS-A.

Our hypothesis that *AdamTS-A* functions to detach cells from the apical ECM during collective migration would be a novel function for this family of proteases. Studies of worm GON-1 in collective gonad migration support its role in clearing a path at the front. The failure of the gonads to migrate in the absence of *gon-1* is completely rescued by expressing GON-1 in only the distal tip cell (Blelloch and Kimble, 1999; Blelloch et al., 1999), a finding that is difficult to reconcile with worm GON-1 functioning in cell detachment. These two different activities can be explained by differences in which side of the cell secretes the protease and potential differences in substrates. Discovering two different activities raises the issue of how ADAMTS-A functions in cells that migrate as individuals. Although many GCs and CVM cells do mis-migrate in *Drosophila AdamTS-A* mutants, many cells in both populations migrate correctly. This suggests no general problems in interpreting and following navigation cues but, instead, a problem in the mechanics of migration, consistent with a role for *Drosophila* ADAMTS-A at either the leading or lagging edge of individual migrating cells. If detachment were delayed, cells might miss short-lived migration cues and follow an aberrant path. Conversely, if failure to clear the path is the problem, cells might instead follow the path of least resistance and end up at the wrong place. Thus, our data do not distinguish between the two proposed mechanisms for ADAMTS-A action in individually migrating cells.

Removing Cad99C suppressed the SG defects in *AdamTS-A* mutants; our biochemical data indicate, however, that Cad99C is not a substrate for ADAMTS-A cleavage. We propose that ADAMTS-A may instead cleave the secreted ECM protein(s) to which Cad99C is thought to bind to link SG cells to the apical matrix (Fig. 7). This idea is consistent with studies of mammalian ADAMTS proteins and worm GON-1, where both known and suspected substrates are secreted proteins: aggrecan, brevican, versican and procollagen for mammalian ADAMTS family members, and Collagen IV and/or Fibulin for GON-1 (Rodriguez-Manzaneque et al., 2002; Sandy et al., 2001; Zheng et al., 2001; Kubota et al., 2004; Lee et al., 2005; McCulloch et al., 2009; Enomoto et al., 2010). Indeed, it appears that it is the closely related ADAM proteases that localize and function at the plasma membrane, and specialize in cleaving transmembrane proteins, including members of the cadherin and protocadherin family. ADAM10 cleaves E-Cadherin (Maretzky et al., 2005; Solanas et al., 2011) and Protocadherin 12 (PCDH12) (Bouillot et al., 2011). Similarly, ADAM13 cleaves Cadherin 11 (McCusker et al., 2009). In addition to cadherins, ADAM10 also cleaves Notch in both vertebrates and flies (Bozkulak and Weinmaster, 2009; Wang et al., 2007), and Robo in flies during axon outgrowth (Coleman et al., 2010). Thus, our data are consistent with the idea that secreted ADAMTS proteases cleave secreted ECM proteins, whereas the closely related transmembrane ADAM proteases cleave transmembrane substrates.

Substrates for *Drosophila* ADAMTS-A may depend on cell type. Indeed, a single mammalian ADAMTS can cleave a variety of targets. For example, ADAMTS 1 cleaves aggrecan, versican or procollagen 1 in a tissue-specific manner (Rodriguez-Manzaneque et al., 2002; Sandy et al., 2001; Lee et al., 2005). Different mammalian ADAMTSs can also cleave the same target protein; ADAMTS 1, ADAMTS 4, ADAMTS 5, ADAMTS 9 and ADAMTS 20 have all been shown to cleave versican in different developmental contexts (Sandy et al., 2001; McCulloch et al., 2009; Enomoto et al., 2010). The fly genome does not encode identifiable aggrecan, brevican or versican homologs, although a clear fibulin homolog exists based on blast searches with the mouse or *C. elegans* proteins (supplementary material Fig. S9A). Interestingly, the *fibulin* gene (*CG31999*) is expressed in embryonic tissues, including the VM, the tissue upon which many of the cell types affected by loss of *AdamTS-A* migrate (supplementary material Fig. S9B-E). Similarly, there are two canonical Collagen I proteins, both expressed and secreted by hemocytes as they migrate throughout the embryo. Identifying the substrates for ADAMTS-A in the SG and other cells that require its activity should provide excellent tools for clarifying the roles of each of the domains of the ADAMTS proteins and provide insight into the role of cell-ECM interactions in development and disease.

**Acknowledgements**

We thank G. Berry, R. Fox, C. Hanlon and two anonymous reviewers for critiquing the manuscript. We thank the Bloomington Stock Center, M. Frasch, S. Hayashi and N. Perrimon for fly stocks, and D. Cavener, R. Cohen, D. Godt and H. Kramer for antisera. We thank FlyBase for information on *AdamTS-A* gene structure and that of the neighboring genes.

**Funding**

This study was funded by the National Institutes of Health National Institute of Dental and Craniofacial Research (NIDCR) [grant number RO1 DE012873 to D.J.A.]. Deposited in PMC for release after 12 months.

**Competing interests statement**

The authors declare no competing financial interests.

**Supplementary material**

Supplementary material available online at
http://dev.biologists.org/lookup/suppl/doi:10.1242/dev.087908/-/DC1

**References**


**Abbaszade, I., Liu, R. Q., Yang, F., Rosenfeld, S. A., Ross, O. H., Link, J. R., Ellis, D. M., Tortorella, M. D., Pratta, M. A., Hollis, J. M. et al.** (1999). Cloning and characterization of ADAMTS11, an aggrecanase from the ADAMTS family. *J. Biol. Chem.* **274**, 23443-23450.

**Abrams, E. W., Mihoulides, W. K. and Andrew, D. J.** (2006). Fork head and Sage maintain a uniform and patent salivary gland lumen through regulation of two downstream target genes, PH4alphaSG1 and PH4alphaSG2. *Development* **133**, 3517-3527.

**Alberts, B., Johnson, A., Lewis, J., Raff, M., Roberst, K. and Walter, P.** (2002). *Molecular Biology of the Cell,* 4th edn. New York, NY: Garland Science.

**Apte, S. S.** (2004). A disintegrin-like and metalloprotease (reprolysin type) with thrombospondin type 1 motifs: the ADAMTS family. *Int. J. Biochem. Cell Biol.* **36**, 981-985.

**Azpiazu, N. and Frasch, M.** (1993). tinman and bagpipe: two homeo box genes that determine cell fates in the dorsal mesoderm of Drosophila. *Genes Dev.* **7**, 1325-1340.

**Blelloch, R. and Kimble, J.** (1999). Control of organ shape by a secreted metalloprotease in the nematode Caenorhabditis elegans. *Nature* **399**, 586-590.

**Blelloch, R., Anna-Arriola, S. S., Gao, D., Li, Y., Hodgkin, J. and Kimble, J.** (1999). The gon-1 gene is required for gonadal morphogenesis in Caenorhabditis elegans. *Dev. Biol.* **216**, 382-393.

**Boswell, R. E. and Mahowald, A. P.** (1985). tudor, a gene required for assembly of the germ plasm in Drosophila melanogaster. *Cell* **43**, 97-104.

**Boube, M., Martin-Bermudo, M. D., Brown, N. H. and Casanova, J.** (2001). Specific tracheal migration is mediated by complementary expression of cell surface proteins. *Genes Dev.* **15**, 1554-1562.

**Bouillot, S., Tillet, E., Carmona, G., Prandini, M. H., Gauchez, A. S., Hoffmann, P., Alfaidy, N., Cand, F. and Huber, P.** (2011). Protocadherin-12 cleavage is a regulated process mediated by ADAM10 protein: evidence of shedding up-regulation in pre-eclampsia. *J. Biol. Chem.* **286**, 15195-15204.

**Bozkulak, E. C. and Weinmaster, G.** (2009). Selective use of ADAM10 and ADAM17 in activation of Notch1 signaling. *Mol. Cell. Biol.* **29**, 5679-5695.

**Bradley, P. L., Myat, M. M., Comeaux, C. A. and Andrew, D. J.** (2003). Posterior migration of the salivary gland requires an intact visceral mesoderm and integrin function. *Dev. Biol.* **257**, 249-262.

**Brand, A. H. and Perrimon, N.** (1993). Targeted gene expression as a means of altering cell fates and generating dominant phenotypes. *Development* **118**, 401-415.

**Brand, A. H., Manoukian, A. S. and Perrimon, N.** (1994). Ectopic expression in Drosophila. *Methods Cell Biol.* **44**, 635-654.

**Brocker, C. N., Vasiliou, V. and Nebert, D. W.** (2009). Evolutionary divergence and functions of the ADAM and ADAMTS gene families. *Hum. Genomics* **4**, 43-55.

**Brower, D. L., Brabant, M. C. and Bunch, T. A.** (1995). Role of the PS integrins in Drosophila development. *Immunol. Cell Biol.* **73**, 558-564.

**Brown, N. H.** (2011). Extracellular matrix in development: insights from mechanisms conserved between invertebrates and vertebrates. *Cold Spring Harb. Perspect. Biol.* **3**, 1-13.

**Cheshire, A. M., Kerman, B. E., Zipfel, W. R., Spector, A. A. and Andrew, D. J.** (2008). Kinetic and mechanical analysis of live tube morphogenesis. *Dev. Dyn.* **237**, 2874-2888.

**Chung, S., Vining, M. S., Bradley, P. L., Chan, C. C., Wharton, K. A., Jr and Andrew, D. J.** (2009). Serrano (sano) functions with the planar cell polarity genes to control tracheal tube length. *PLoS Genet.* **5**, e1000746.

**Chung, S., Chavez, C. and Andrew, D. J.** (2011). Trachealess (Trh) regulates all tracheal genes during Drosophila embryogenesis. *Dev. Biol.* **360**, 160-172.

**Coleman, H. A., Labrador, J. P., Chance, R. K. and Bashaw, G. J.** (2010). The Adam family metalloprotease Kuzbanian regulates the cleavage of the roundabout receptor to control axon repulsion at the midline. *Development* **137**, 2417-2426.

**D'Alterio, C., Tran, D. D., Yeung, M. W., Hwang, M. S., Li, M. A., Arana, C. J., Mulligan, V. K., Kubesh, M., Sharma, P., Chase, M. et al.** (2005). Drosophila melanogaster Cad99C, the orthologue of human Usher cadherin PCDH15, regulates the length of microvilli. *J. Cell Biol.* **171**, 549-558.

**Dong, J. F., Moake, J. L., Nolasco, L., Bernardo, A., Arceneaux, W., Shrimpton, C. N., Schade, A. J., McIntire, L. V., Fujikawa, K. and López, J. A.** (2002). ADAMTS-13 rapidly cleaves newly secreted ultralarge von Willebrand factor multimers on the endothelial surface under flowing conditions. *Blood* **100**, 4033-4039.

**Dunn, J. R., Reed, J. E., du Plessis, D. G., Shaw, E. J., Reeves, P., Gee, A. L., Warnke, P. and Walker, C.** (2006). Expression of ADAMTS-8, a secreted protease with antiangiogenic properties, is downregulated in brain tumours. *Br. J. Cancer* **94**, 1186-1193.

**El Hour, M., Moncada-Pazos, A., Blacher, S., Masset, A., Cal, S., Berndt, S., Detilleux, J., Host, L., Obaya, A. J., Maillard, C. et al.** (2010). Higher sensitivity of Adamts12-deficient mice to tumor growth and angiogenesis. *Oncogene* **29**, 3025-3032.

**Enomoto, H., Nelson, C. M., Somerville, R. P., Mielke, K., Dixon, L. J., Powell, K. and Apte, S. S.** (2010). Cooperation of two ADAMTS metalloproteases in closure of the mouse palate identifies a requirement for versican proteolysis in regulating palatal mesenchyme proliferation. *Development* **137**, 4029-4038.

**Fan, Y. and Bergmann, A.** (2010). The cleaved-Caspase-3 antibody is a marker of Caspase-9-like DRONC activity in Drosophila. *Cell Death Differ.* **17**, 537-539.

**Ginsberg, M. H., Du, X. and Plow, E. F.** (1992). Inside-out integrin signalling. *Curr. Opin. Cell Biol.* **4**, 766-771.

**Gong, W. J. and Golic, K. G.** (2003). Ends-out, or replacement, gene targeting in Drosophila. *Proc. Natl. Acad. Sci. USA* **100**, 2556-2561.

**Gullberg, D. and Ekblom, P.** (1995). Extracellular matrix and its receptors during development. *Int. J. Dev. Biol.* **39**, 845-854.

**Häcker, U., Kaufmann, E., Hartmann, C., Jürgens, G., Knöchel, W. and Jäckle, H.** (1995). The Drosophila fork head domain protein crocodile is required for the establishment of head structures. *EMBO J.* **14**, 5306-5317.

**Held-Feindt, J., Paredes, E. B., Blömer, U., Seidenbecher, C., Stark, A. M., Mehdorn, H. M. and Mentlein, R.** (2006). Matrix-degrading proteases ADAMTS4 and ADAMTS5 (disintegrins and metalloproteinases with thrombospondin motifs 4 and 5) are expressed in human glioblastomas. *Int. J. Cancer* **118**, 55-61.

**Henderson, K. D. and Andrew, D. J.** (2000). Regulation and function of Scr, exd, and hth in the Drosophila salivary gland. *Dev. Biol.* **217**, 362-374.

**Isaac, D. D. and Andrew, D. J.** (1996). Tubulogenesis in Drosophila: a requirement for the trachealess gene product. *Genes Dev.* **10**, 103-117.

**Ismat, A., Schaub, C., Reim, I., Kirchner, K., Schultheis, D. and Frasch, M.** (2010). HLH54F is required for the specification and migration of longitudinal gut muscle founders from the caudal mesoderm of Drosophila. *Development* **137**, 3107-3117.

**Jones, G. C. and Riley, G. P.** (2005). ADAMTS proteinases: a multi-domain, multi-functional family with roles in extracellular matrix turnover and arthritis. *Arthritis Res. Ther.* **7**, 160-169.

**Jönsson-Rylander, A. C., Nilsson, T., Fritsche-Danielson, R., Hammarström, A., Behrendt, M., Andersson, J. O., Lindgren, K., Andersson, A. K., Wallbrandt, P., Rosengren, B. et al.** (2005). Role of ADAMTS-1 in atherosclerosis: remodeling of carotid artery, immunohistochemistry, and proteolysis of versican. *Arterioscler. Thromb. Vasc. Biol.* **25**, 180-185.

**Kerman, B. E., Cheshire, A. M. and Andrew, D. J.** (2006). From fate to function: the Drosophila trachea and salivary gland as models for tubulogenesis. *Differentiation* **74**, 326-348.

**Kerman, B. E., Cheshire, A. M., Myat, M. M. and Andrew, D. J.** (2008). Ribbon modulates apical membrane during tube elongation through Crumbs and Moesin. *Dev. Biol.* **320**, 278-288.

**Kessenbrock, K., Plaks, V. and Werb, Z.** (2010). Matrix metalloproteinases: regulators of the tumor microenvironment. *Cell* **141**, 52-67.

**Knirr, S., Azpiazu, N. and Frasch, M.** (1999). The role of the NK-homeobox gene slouch (S59) in somatic muscle patterning. *Development* **126**, 4525-4535.

**Kubota, Y., Kuroki, R. and Nishiwaki, K.** (2004). A fibulin-1 homolog interacts with an ADAM protease that controls cell migration in C. elegans. *Curr. Biol.* **14**, 2011-2018.

**Kunwar, P. S., Siekhaus, D. E. and Lehmann, R.** (2006). In vivo migration: a germ cell perspective. *Annu. Rev. Cell Dev. Biol.* **22**, 237-265.

**Lee, N. V., Rodriguez-Manzaneque, J. C., Thai, S. N., Twal, W. O., Luque, A., Lyons, K. M., Argraves, W. S. and Iruela-Arispe, M. L.** (2005). Fibulin-1 acts as a cofactor for the matrix metalloprotease ADAMTS-1. *J. Biol. Chem.* **280**, 34796-34804.

**Llamazares, M., Cal, S., Quesada, V. and López-Otín, C.** (2003). Identification and characterization of ADAMTS-20 defines a novel subfamily of metalloproteinases-disintegrins with multiple thrombospondin-1 repeats and a unique GON domain. *J. Biol. Chem.* **278**, 13382-13389.

**Maretzky, T., Reiss, K., Ludwig, A., Buchholz, J., Scholz, F., Proksch, E., de Strooper, B., Hartmann, D. and Saftig, P.** (2005). ADAM10 mediates E-cadherin shedding and regulates epithelial cell-cell adhesion, migration, and beta-catenin translocation. *Proc. Natl. Acad. Sci. USA* **102**, 9182-9187.

**Martin, D., Zusman, S., Li, X., Williams, E. L., Khare, N., DaRocha, S., Chiquet-Ehrismann, R. and Baumgartner, S.** (1999). wing blister, a new Drosophila laminin alpha chain required for cell adhesion and migration during embryonic and imaginal development. *J. Cell Biol.* **145**, 191-201.

**Maruyama, R. and Andrew, D. J.** (2012). Drosophila as a model for epithelial tube formation. *Dev. Dyn.* **241**, 119-135.

**McCulloch, D. R., Nelson, C. M., Dixon, L. J., Silver, D. L., Wylie, J. D., Lindner, V., Sasaki, T., Cooley, M. A., Argraves, W. S. and Apte, S. S.** (2009). ADAMTS metalloproteases generate active versican fragments that regulate interdigital web regression. *Dev. Cell* **17**, 687-698.

**McCusker, C., Cousin, H., Neuner, R. and Alfandari, D.** (2009). Extracellular cleavage of cadherin-11 by ADAM metalloproteases is essential for Xenopus cranial neural crest cell migration. *Mol. Biol. Cell* **20**, 78-89.

**Murphy, G.** (2008). The ADAMs: signalling scissors in the tumour microenvironment. *Nat. Rev. Cancer* **8**, 929-941.
**Myat, M. M. and Andrew, D. J.** (2000). Fork head prevents apoptosis and promotes cell shape change during formation of the Drosophila salivary glands. *Development* **127**, 4217-4226.
**Myat, M. M. and Andrew, D. J.** (2002). Epithelial tube morphology is determined by the polarized growth and delivery of apical membrane. *Cell* **111**, 879-891.
**Nakada, M., Miyamori, H., Kita, D., Takahashi, T., Yamashita, J., Sato, H., Miura, R., Yamaguchi, Y. and Okada, Y.** (2005). Human glioblastomas overexpress ADAMTS-5 that degrades brevican. *Acta Neuropathol.* **110**, 239-246.
**Nelson, C. R. and Szauter, P.** (1992). Cytogenetic analysis of chromosome region 89A of Drosophila melanogaster: isolation of deficiencies and mapping of Po, Aldox-1 and transposon insertions. *Mol. Gen. Genet.* **235**, 11-21.
**Nishiwaki, K., Hisamoto, N. and Matsumoto, K.** (2000). A metalloprotease disintegrin that controls cell migration in Caenorhabditis elegans. *Science* **288**, 2205-2208.
**Ozdowski, E. F., Mowery, Y. M. and Cronmiller, C.** (2009). Stall encodes an ADAMTS metalloprotease and interacts genetically with Delta in Drosophila ovarian follicle formation. *Genetics* **183**, 1027-1040.
**Pirraglia, C., Waters, J. and Myat, M.M.** (2010). Pak1 control of E-cadherin endocytosis regulates salivary gland lumen size and shape. *Development* **137**, 4177-4189.
**Reuter, R. and Scott, M. P.** (1990). Expression and function of the homoeotic genes Antennapedia and Sex combs reduced in the embryonic midgut of Drosophila. *Development* **109**, 289-303.
**Rodríguez-Manzaneque, J. C., Westling, J., Thai, S. N., Luque, A., Knauper, V., Murphy, G., Sandy, J. D. and Iruela-Arispe, M. L.** (2002). ADAMTS1 cleaves aggrecan at multiple sites and is differentially inhibited by metalloproteinase inhibitors. *Biochem. Biophys. Res. Commun.* **293**, 501-508.
**Rørth, P.** (2009). Collective cell migration. *Annu. Rev. Cell Dev. Biol.* **25**, 407-429.
**Rozario, T. and DeSimone, D. W.** (2010). The extracellular matrix in development and morphogenesis: a dynamic view. *Dev. Biol.* **341**, 126-140.
**Sandy, J. D., Westling, J., Kenagy, R. D., Iruela-Arispe, M. L., Verscharen, C., Rodriguez-Mazaneque, J. C., Zimmermann, D. R., Lemire, J. M., Fischer, J. W., Wight, T. N. et al.** (2001). Versican V1 proteolysis in human aorta in vivo occurs at the Glu441-Ala442 bond, a site that is cleaved by recombinant ADAMTS-1 and ADAMTS-4. *J. Biol. Chem.* **276**, 13372-13378.
**Sastry, S. K. and Horwitz, A. F.** (1993). Integrin cytoplasmic domains: mediators of cytoskeletal linkages and extra- and intracellular initiated transmembrane signaling. *Curr. Opin. Cell Biol.* **5**, 819-831.
**Satoh, A. K., O'Tousa, J. E., Ozaki, K. and Ready, D. F.** (2005). Rab11 mediates post-Golgi trafficking of rhodopsin to the photosensitive apical membrane of Drosophila photoreceptors. *Development* **132**, 1487-1497.
**Schwartz, M. A.** (1992). Transmembrane signalling by integrins. *Trends Cell Biol.* **2**, 304-308.
**Shiga, Y., Tanaka-Matakatsu, M. and Hayashi, S.** (1996). A nuclear GFP/β-galactosidase fusion protein as a marker for morphogenesis in living Drosophila. *Dev. Growth Differ.* **38**, 99-106.
**Silver, D. L., Hou, L., Somerville, R., Young, M. E., Apte, S. S. and Pavan, W. J.** (2008). The secreted metalloprotease ADAMTS20 is required for melanoblast survival. *PLoS Genet.* **4**, e1000003.
**Solanas, G., Cortina, C., Sevillano, M. and Batlle, E.** (2011). Cleavage of E-cadherin by ADAM10 mediates epithelial cell sorting downstream of EphB signalling. *Nat. Cell Biol.* **13**, 1100-1107.
**Somerville, R. P., Longpre, J. M., Jungers, K. A., Engle, J. M., Ross, M., Evanko, S., Wight, T. N., Leduc, R. and Apte, S. S.** (2003). Characterization of ADAMTS-9 and ADAMTS-20 as a distinct ADAMTS subfamily related to Caenorhabditis elegans GON-1. *J. Biol. Chem.* **278**, 9503-9513.
**Starz-Gaiano, M. and Montell, D. J.** (2004). Genes that drive invasion and migration in Drosophila. *Curr. Opin. Genet. Dev.* **14**, 86-91.
**Streuli, C.** (1999). Extracellular matrix remodelling and cellular differentiation. *Curr. Opin. Cell Biol.* **11**, 634-640.
**Van Doren, M., Broihier, H. T., Moore, L. A. and Lehmann, R.** (1998). HMG-CoA reductase guides migrating primordial germ cells. *Nature* **396**, 466-469.
**Vázquez, F., Hastings, G., Ortega, M. A., Lane, T. F., Oikemus, S., Lombardo, M. and Iruela-Arispe, M. L.** (1999). METH-1, a human ortholog of ADAMTS-1, and METH-2 are members of a new family of proteins with angio-inhibitory activity. *J. Biol. Chem.* **274**, 23349-23357.
**Vining, M. S., Bradley, P. L., Comeaux, C. A. and Andrew, D. J.** (2005). Organ positioning in Drosophila requires complex tissue-tissue interactions. *Dev. Biol.* **287**, 19-34.
**Vu, T. H. and Werb, Z.** (2000). Matrix metalloproteinases: effectors of development and normal physiology. *Genes Dev.* **14**, 2123-2133.
**Wang, X., Adam, J. C. and Montell, D.** (2007). Spatially localized Kuzbanian required for specific activation of Notch during border cell migration. *Dev. Biol.* **301**, 532-540.
**Wilcox, M., DiAntonio, A. and Leptin, M.** (1989). The function of PS integrins in Drosophila wing morphogenesis. *Development* **107**, 891-897.
**Wolf, K. and Friedl, P.** (2011). Extracellular matrix determinants of proteolytic and non-proteolytic cell migration. *Trends Cell Biol.* **21**, 736-744.
**Xu, N., Keung, B. and Myat, M. M.** (2008). Rho GTPase controls invagination and cohesive migration of the Drosophila salivary gland through Crumbs and Rho-kinase. *Dev. Biol.* **321**, 88-100.
**Zheng, X., Chung, D., Takayama, T. K., Majerus, E. M., Sadler, J. E. and Fujikawa, K.** (2001). Structure of von Willebrand factor-cleaving protease (ADAMTS13), a metalloprotease involved in thrombotic thrombocytopenic purpura. *J. Biol. Chem.* **276**, 41059-41063.